Proton MRI of Lung Parenchyma Reflects Allergen-Induced Airway Remodeling and Endotoxin-Aroused Hyporesponsiveness: A Step Toward Ventilation Studies in Spontaneously Breathing Rats

Nicolau Beckmann,[1*] Catherine Cannet,[2] Stefan Zurbruegg,[1] Markus Rudin,[1] and Bruno Tigani[1]

Proton signals from lung parenchyma were detected with the use of a gradient-echo sequence to noninvasively obtain information on pulmonary function in models of airway diseases in rats. Initial measurements carried out in artificially ventilated control rats revealed a highly significant negative correlation between the parenchymal signal and the partial pressure of oxygen (pO_2) in the blood, for different amounts of oxygen administered. The magnitude of the signal intensity variations caused by changes in the oxygen concentration was larger than expected solely from the paramagnetic properties of molecular oxygen. Inhomogeneous line-broadening induced by lung inflation may explain the observed signal amplification. Experiments carried out in spontaneously breathing animals challenged with allergen or endotoxin revealed parenchymal signal changes that reflected the oxygenation status of the lungs and were consistent with airway remodeling or hyporesponsiveness. The results suggest that proton MRI of parenchymal tissue is a sensitive tool for probing the functional status of the lung in rat models of respiratory diseases. The method is complementary to the recently described noninvasive assessment by MRI of pulmonary inflammation in small rodents. Overall, these techniques provide invaluable information for profiling anti-inflammatory drugs in models of airway diseases. Magn Reson Med 52:258–268, 2004. **© 2004 Wiley-Liss, Inc.**

Key words: airway remodeling; asthma; chronic obstructive pulmonary disease (COPD); lung; lung ventilation; magnetic resonance imaging (MRI); oxygen-enhanced MRI; rat; ventilation

Several animal models have been developed in an attempt to mimic and study specific aspects of human respiratory diseases (1,2). For instance, actively sensitized Brown Norway (BN) rats exposed to allergens develop airway hyperresponsiveness and an eosinophilic inflammation together with an increase in activated T cells (CD25+) in the airways (3,4), and thus manifest some key features of asthmatic inflammation. Also, an inflammation that shows some characteristics of chronic obstructive pulmonary disease (COPD) can be elicited in rodents by the administration of endotoxin (lipopolysaccharide (LPS)), a bacterial macromolecular cell surface antigen (5,6).

In pharmacological studies of pulmonary inflammation at the preclinical level, histology and analysis of bronchoalveolar lavage fluid are routinely used to assess the inflammatory status of the lung and the results of drug intervention. Although they provide comprehensive information at the cellular level, these methods have the drawback of being terminal. It was recently shown that proton MRI can be used to noninvasively characterize the inflammatory status of the rat lungs following allergen (7) or endotoxin (8) challenge. The significant correlation between the MRI signals and the perivascular edema determined by histology provides a basis for the noninvasive assessment of a key component of inflammation in the allergen model (9). With this approach, one can assess the rapid effects of drugs in vivo by monitoring the rate at which edematous signals resolve. In addition, the prospect of using MRI to noninvasively detect a sustained mucus hypersecretory phenotype induced by endotoxin brings an important new perspective to models of COPD in animals.

Inflammation in airways leads to pathophysiologic changes in the structure of the lung tissue, including thickening of the smooth muscle in the airway wall (10), which can influence airway responsiveness (11), as well as ventilation. The progressive structural change known as airway remodeling, which is driven by chronic local inflammation, is a fundamental component in the development of irreversible airway hyperresponsiveness (for a recent review, see Ref. 12).

The aim of the present work was to monitor noninvasively by MRI the effects of airway remodeling and hyporesponsiveness following allergen or endotoxin challenges, respectively, in the rat. We used a gradient-echo sequence, as described in Ref. 13, to detect modulations of proton signals from lung parenchyma induced by changes in oxygenation levels. Molecular oxygen is weakly paramagnetic, and this property has been explored to derive ventilation-related information from the human lung (14–18). Since airway remodeling can influence ventilation, and ventilation is automatically impaired in regions containing edema, we were interested in probing the function of tissue in areas devoid of edematous responses. Initial data were obtained in artificially ventilated rats to verify the reliability of the technique in detecting the effects on parenchymal signal caused by differences in oxygen con-

[1]Discovery Technologies Center, Novartis Institutes for BioMedical Research, Basel, Switzerland.

[2]Transplantation Research, Novartis Institutes for BioMedical Research, Basel, Switzerland.

Grant sponsor: 3R Research Foundation, Muensinger, Switzerland; Grant number: 82-002 (to NB).

*Correspondence to: Nicolau Beckmann, Ph.D., Novartis Institutes for BioMedical Research, Discovery Technologies, Analytics and Imaging Sciences Unit, Lichstr. 35, WSJ-386.2.09, CH-4002 Basel, Switzerland. E-mail: nicolau.beckmann@pharma.novartis.com

Received 8 January 2004; revised 18 February 2004; accepted 23 February 2004.

DOI 10.1002/mrm.20127
Published online in Wiley InterScience (www.interscience.wiley.com).

© 2004 Wiley-Liss, Inc.

tent of the administered gas. Thereafter, measurements were obtained in spontaneously breathing animals.

MATERIALS AND METHODS

The experiments were carried out according to the Swiss federal regulations for animal protection.

Animals

Male BN rats (Iffa-Credo, L'Arbresle, France) weighing approximately 250 g were used throughout the study. They were housed in a temperature- and humidity-controlled environment, with free access to standard rat chow and tap water.

Allergen Challenge

Sensitization Protocol

Ovalbumin (OVA, 20 μg/ml; Fluka, Buchs, Switzerland) was mixed with aluminum hydroxide (20 mg/ml) and injected (0.5 ml per animal s.c.) on days 1, 15, and 22.

Allergen Exposure

On day 29, the animals were anesthetized with 4% isoflurane (Abbott, Cham, Switzerland). OVA (0.3 mg/kg dissolved in 0.2 ml saline) or vehicle (saline, 0.2 ml per animal) was administered intratracheally (i.t.) and the animals were allowed to recover.

Endotoxin Challenge

Naïve rats were anesthetized with 4% isoflurane. Then LPS from *Salmonella typhosa* (1 ml/kg; Sigma, Dorset, UK) dissolved in 0.2 ml saline or vehicle (saline, 0.2 ml) was administered i.t., and the animals were allowed to recover. Some animals were treated with the nitric oxide synthase inhibitor N^G-nitro-L-arginine methyl ester (L-NAME, 10 mg/kg i.v.; Sigma) 10 min before the challenge.

Animal Preparation for MRI Measurements

During the MRI acquisitions, the animals were placed in a supine position in a cradle made of Plexiglas. Body temperature was maintained at 37°C ± 1°C by warm air, and regulated by a rectal temperature probe (DM 852; Ellab, Copenhagen, Denmark).

Spontaneously Breathing Animals

The rats were anesthetized with 2.5% isoflurane in a mixture of O_2/N_2 (21% O_2) administered via a face mask.

Ventilated Animals

The rats were anesthetized with an initial dose of 3% isoflurane in O_2/N_2 (1:2), intubated with a cannula made from polyethylene (internal diameter = 0.4 mm; outer diameter = 0.8 mm), and artificially ventilated with a small-animal ventilator (KTR3, Alfos Electronics, Switzerland). For maintenance, the isoflurane was set to 2.5% and the respiration rate was kept at 60 beats/min. After the animals were anesthetized, they were given an intramuscular injection of vecuronium bromide (12 mg/kg; Sigma) to suppress spontaneous respiration. We monitored blood gases (O_2 and CO_2) during some of the experiments by drawing blood samples (100 μl) from a catheter placed in the femoral artery. The blood was then analyzed by means of a blood gas analyzer (IL Synthesis 35; Instrumentation Laboratory AG, Schlieren, Switzerland).

MRI

Measurements were carried out with a Biospec 47/40 spectrometer (Bruker Medical Systems, Karlsruhe, Germany) operating at 4.7 T, equipped with an actively shielded gradient system capable of generating a gradient of 200 mT/m. The operational software of the scanner was Paravision (Bruker). A birdcage resonator of 7 cm diameter was used for excitation and detection. The parameters of a gradient-echo sequence were chosen with the aim of detecting either lung parenchyma (13) or signals appearing in the lung after an allergen or endotoxin challenge (7,8).

Lung Parenchyma

The rise time of the gradient was set to 60 μs, and the following parameters were used: matrix size = 36 × 128, field of view (FOV) = 6 × 6 cm^2, slice thickness = 2 mm, excitation pulse (Gaussian shape) length = 250 μs, flip angle = ~15°, repetition time (TR) = 1.95 ms, and echo time (TE) = 545 μs. The acquisition of an individual image took 250 ms. We obtained a single-slice image by computing the 2DFT of the averaged signal from N individual image acquisitions, and interpolating the data set to 256 × 256 pixels. There was an interval of 500 ms between individual image acquisitions. Thus, for N = 40 averages, for instance, the total acquisition time for a single slice was 30 s. The position of the slice was chosen to avoid as much as possible regions containing edematous signals.

Reported parenchymal signal intensities correspond to mean values over five images acquired consecutively. The parenchymal signal was calibrated with the external muscle used as reference. The coefficient of variation of the muscle signal was <1%. In experiments in which the gas composition was changed, the minimum interval of time between the composition change and the image acquisition was of 3 min.

T_2^* Assessment

To assess the T_2^* of parenchymal tissue, we acquired a series of axial images with the following TEs: 1120 μs, 890 μs, 750 μs, 660 μs, 600 μs, 560 μs, 520 μs, and 505 μs. The number of averages was 80, and TR was kept constant at 4.3 ms. The acquisition time for one image was 44 s. Average signal intensities were determined for regions of interest (ROIs) located in the peripheral lung to avoid the effects of blood flow within the larger pulmonary vessels. The ratio between the average signal intensity in a portion of the lung and in the muscle for several TEs was fitted to an exponential decay [$\exp(-TE/T_2^*)$].

Assessment of Edematous Signals

The following parameters were used: TR = 5.6 ms, TE = 2.7 ms, excitation pulse (Gaussian shape) length = 1 ms,

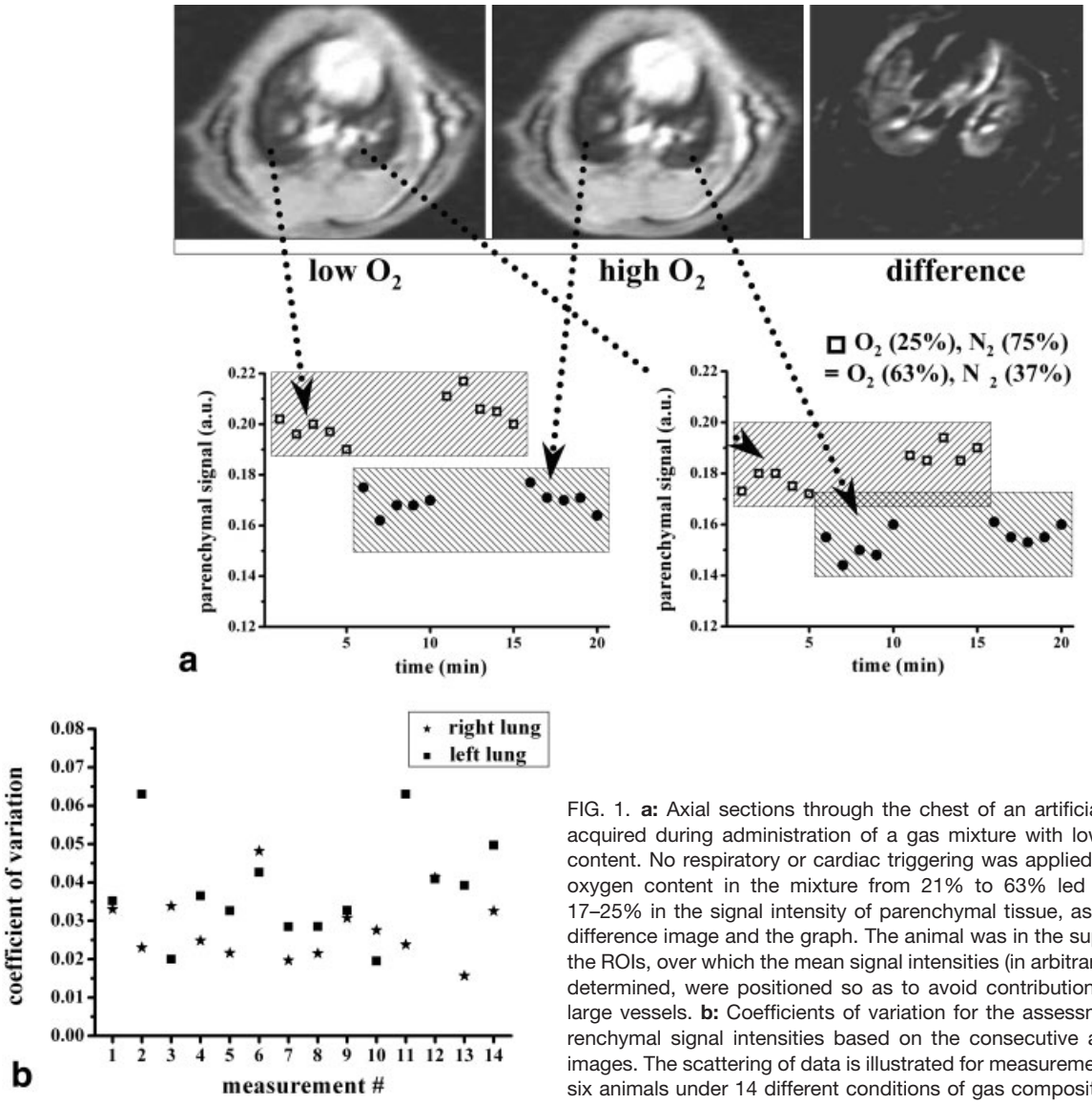


FIG. 1. **a:** Axial sections through the chest of an artificially ventilated rat, acquired during administration of a gas mixture with low or high oxygen content. No respiratory or cardiac triggering was applied. A change of the oxygen content in the mixture from 21% to 63% led to differences of 17–25% in the signal intensity of parenchymal tissue, as illustrated by the difference image and the graph. The animal was in the supine position, and the ROIs, over which the mean signal intensities (in arbitrary units, a.u.) were determined, were positioned so as to avoid contributions of signals from large vessels. **b:** Coefficients of variation for the assessment of mean parenchymal signal intensities based on the consecutive acquisition of five images. The scattering of data is illustrated for measurements carried out on six animals under 14 different conditions of gas composition.

flip angle of the excitation pulse = ~15°, FOV = 6 × 6 cm^2, matrix size = 256 × 128, and slice thickness = 1.5 mm. We obtained a single-slice image by computing the 2DFT of the averaged signal from 40 individual image acquisitions, and interpolating the data set to 256 × 256 pixels. There was an interval of 530 ms between individual image acquisitions, resulting in a total acquisition time of 50 s for a single slice. The entire lung was covered by 28 consecutive slices.

Image Analysis

The volume of signals appearing in the lung following OVA or LPS challenge was quantified with the use of a semiautomatic segmentation procedure (described in detail in Ref. 7). The segmentation parameters were the same for all of the analyzed images, and were chosen to segment regions corresponding to high-intensity signals. Since the intensity of the lung signals due to allergen or endotoxin challenge was comparable to that of the vessels, the volume corresponding to the vessels was assessed on baseline images and then subtracted from the volumes determined on post-challenge images.

Histology

Immediately after the MRI acquisitions, actively sensitized BN rats were killed with an overdose of pentobarbital (250 mg/kg i.p.). The lungs were fixed by slow in situ inflation with approximately 5 ml of 10% phosphate-buffered neutral formalin (BNF), pH 7.2, via a tracheal cannula. After the lungs were removed from the thorax, they were kept in BNF for a maximum period of 72 hr. Following fixation, the lungs were trimmed and sections were cut longitudinally through the left lobe and transversally through the right caudal lobe so as to include the main bronchi as well as the pulmonary alveoli. The sections were then embedded in paraffin blocks. Sections (3 μm thick) of each block were stained with 1) PAS/Alcian blue for identification and counting of goblet cells, and measurements of bronchial epithelial thickness; and 2) hematoxylin and eosin for morphometric analyses of the air-

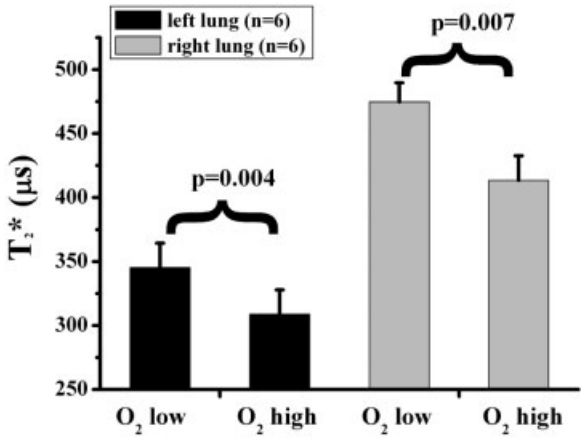


FIG. 2. T_2^* of lung parenchymal tissue (mean ± SEM) in the left and right lungs under low (21%) and high (63%) oxygen content in the inhaled mixture of gas, for artificially ventilated rats in the supine position.

ways. The sections were immunostained for smooth muscle actin (DAKO A/S, Glostrup, Denmark) and labeled with an avidin biotin peroxidase diaminobenzidine system for quantification of the peribronchial smooth muscle area. All sections were examined in a blind manner with a light microscope (DMR BE; Leica Microsystems, Glattbrugg, Switzerland) connected to a video camera (ProgRes/3008; Jenoptic LOS, Eching, Germany). The morphometric analyses were performed with the image analysis software Image Access 3.10 (IMAGIC, Glattbrugg, Switzerland).

To count the goblet cells and assess bronchial thickness, we captured images of 13 intrapulmonary bronchi (nine of the left lobe and four of the right one) at ×100 magnification. Bronchi having basement membrane diameters (external epithelial diameters) ranging from 150 to 450 μm were selected. All goblet cells of each bronchus were counted. The basal laminae and the airway lumen were manually circumscribed, and the external and internal bronchial areas were calculated. The bronchial epithelial thickness was calculated from these two areas, under the assumption that the bronchial sections were round.

The airways area was quantified on five consecutive images captured from the left lobe at ×50 magnification. The program produced a binary black and white image, and the percentage of the white area, corresponding to the airways area, was then automatically calculated.

For the peribronchial smooth muscle measurement, images of three intrapulmonary bronchi of the left lobe were captured at ×100 magnification. Bronchi with basement membrane (external epithelial) diameters ranging from 200 to 400 μm were selected for evaluation. The ratio between the area of peribronchial smooth muscle circumscribed manually and the bronchus diameter was calculated.

Statistics

The mean values (±SEM) from *N* individual animals are presented. Student's *t*-tests or analysis of variance (ANOVA) multiple-comparison tests with Bonferroni correction were carried out. Significance was assumed at the 5% probability level.

RESULTS

Artificially Ventilated Rats

Figure 1 shows transverse sections through the chest of an artificially ventilated rat, acquired under low (21%) and high (63%) oxygen content of the administered gas mixture. The lung parenchymal signal under low oxygen content was 17–25% more intense than under high oxygen ventilation conditions, as illustrated by the difference image. Reproducible signal changes were observed when the composition of the gas was altered from low to high oxygen content or vice versa (Fig. 1a, insert). Furthermore, for a given gas composition, the coefficients of variation for the parenchymal signal intensity assessed from five images acquired consecutively ranged from 1.6% to 6.3% (Fig. 1b).

When the oxygen composition of the inhaled gas was changed from low (21%) to high (63%), there was a sig-

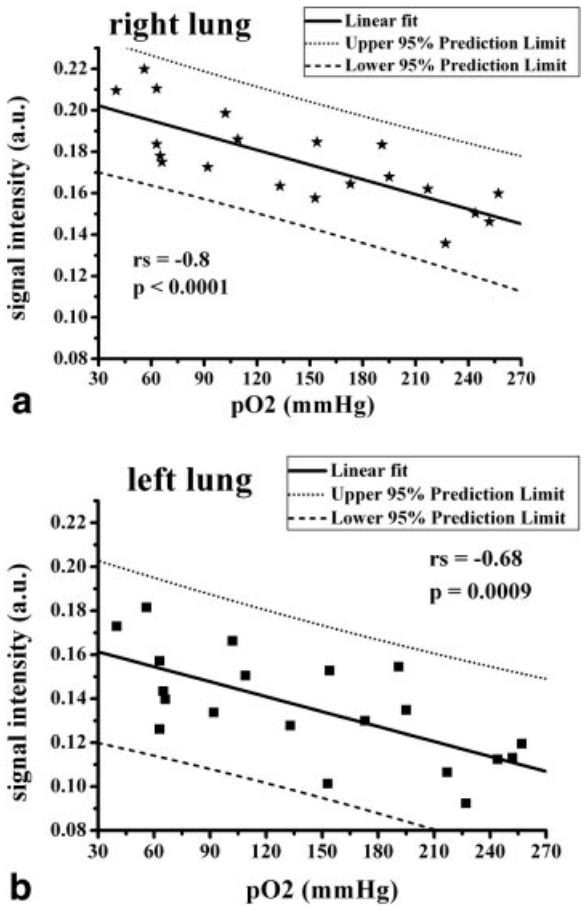


FIG. 3. Correlation between the parenchymal signal intensity of lung images and the pO_2 in the blood. Parenchymal signal values were obtained from 10 artificially ventilated rats, for different oxygen concentrations (minimum: 21%, maximum: 63%) in the inhaled gas mixture. The position of the ROIs, over which the mean signal intensities were determined, was chosen so as to avoid contributions of signals from large vessels.

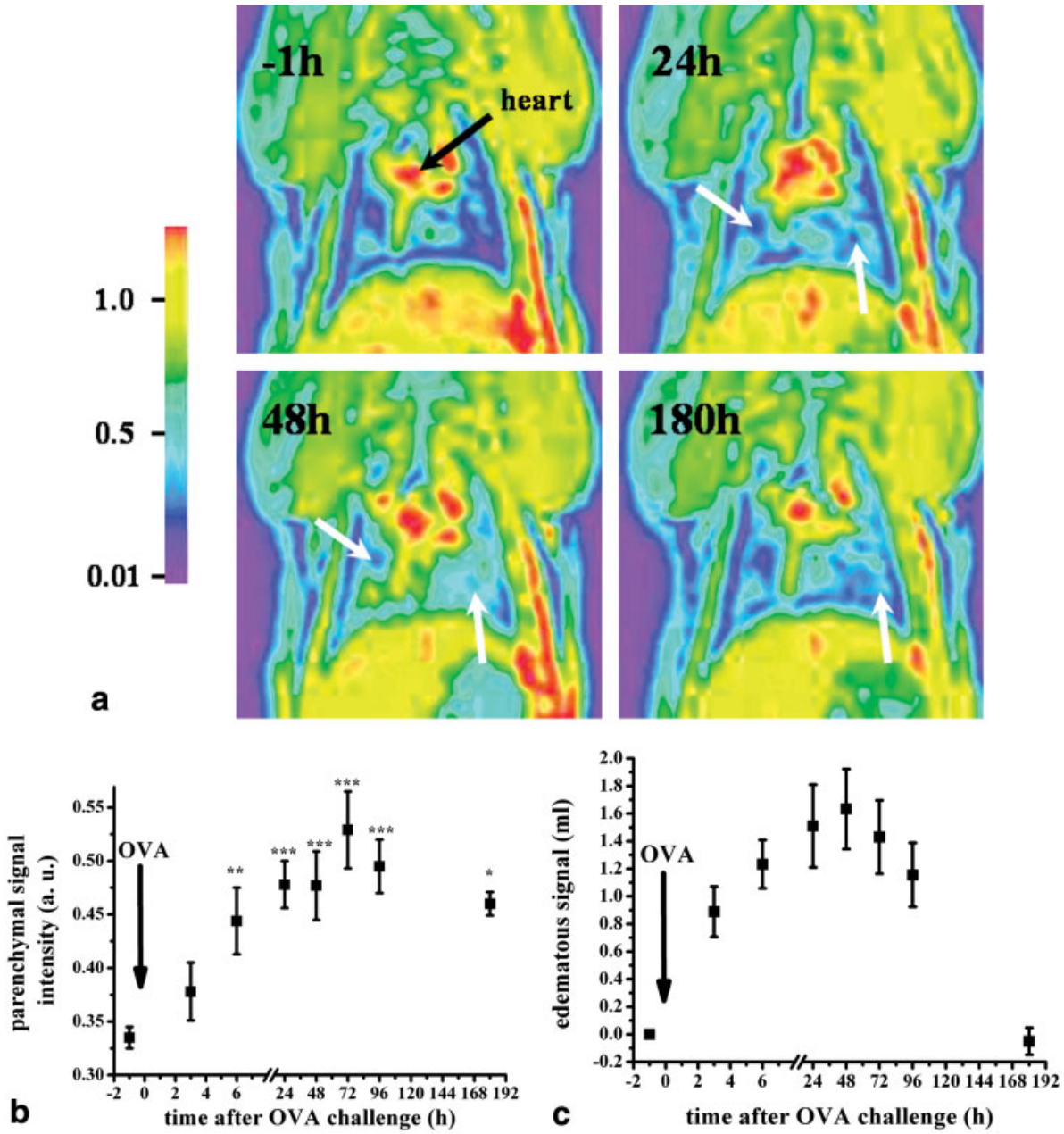


FIG. 4. **a:** Coronal sections acquired through the chest of a rat, before and at several time points after OVA (0.3 mg/kg i.t.) challenge. The position of the slices was chosen to avoid as much as possible regions containing edematous signals. Images are displayed in false color to highlight the parenchymal signal increase post challenge (white arrows). The scale on the left side indicates signal intensity in arbitrary units. **b:** Mean parenchymal signal intensities (±SEM) following OVA administration (0.3 mg/kg i.t.) to actively sensitized rats. The position of the ROIs, over which the signal intensities were determined, was chosen so as to avoid contribution from edematous signals and large vessels. The significance levels correspond to comparisons with baseline (BL) signal intensities, before the challenge (* $0.01 < P < 0.05$; ***$0.0001 < P < 0.001$). **c:** Time course of the volume of edematous signals (mean ± SEM) in lungs of OVA-challenged animals.

nificant reduction in the relaxation time T_2^* of lung parenchyma by approximately 15% (Fig. 2). Coefficients of variation for T_2^* assessments in six different animals were on the order of 10%.

A significant inverse correlation was found between the parenchymal signal intensity in the lung images and the partial pressure of oxygen (pO_2) in the blood, for different amounts of oxygen (minimum: 21%, maximum: 63%) in the administered gas (Fig. 3).

Spontaneously Breathing Rats

The fact that changes in the parenchymal signal intensity were consistently detected when the oxygen content of the administered gas mixture was altered in artificially ventilated rats was used as the basis for deriving functional information regarding the lung in two models of respiratory diseases. Measurements were carried out on spontaneously breathing animals so as to interfere as little as

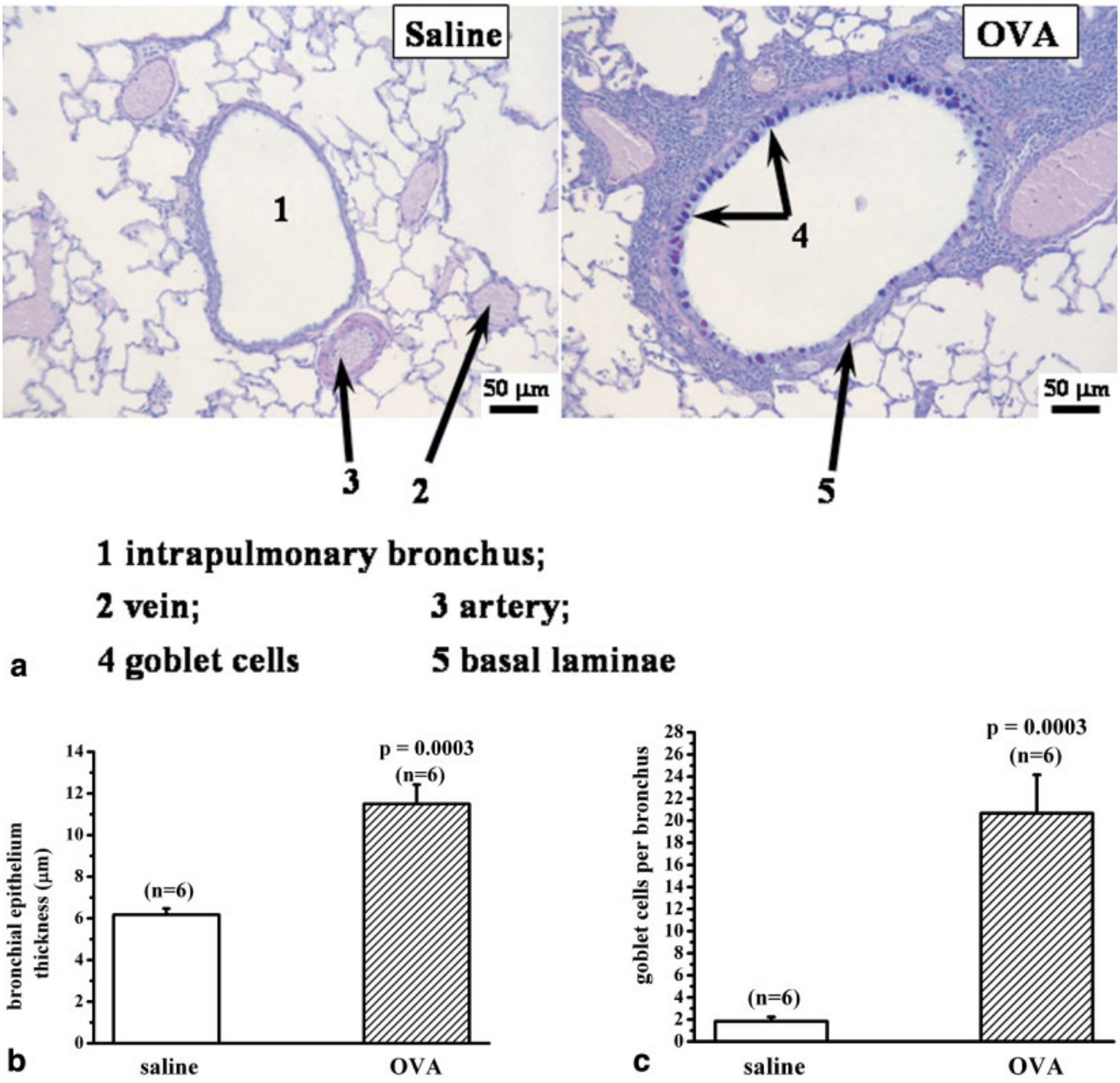


FIG. 5. Continued.

possible with the pathophysiology of the response. The position and shape of the ROIs in which the signal intensities were determined were carefully chosen to avoid contributions from edematous signals and large vessels.

OVA Challenge

Parenchymal signal intensity was significantly increased by 50–70% compared to baseline values from 6 hr to 96 hr after OVA challenge (Fig. 4a and b). A significantly enhanced parenchymal signal, which may be indicative of impaired ventilation following OVA instillation, was still detected 180 hr post-challenge. Repetitive measurements performed on control animals (actively sensitized rats challenged with saline, $N = 12$) at the same time points as those represented in Fig. 4b revealed mean parenchymal signal intensities ranging between 0.34 and 0.39, with variances of 0.003–0.0075 (i.e., comparable to the baseline values obtained before OVA administration). Consistent with previous results (7), the edematous signal volume was maximum at 48 hr, and it completely resolved 180 hr after challenge (Fig. 4c). A significant correlation ($r = 0.59$, $P = 0.002$, $N = 24$) between parenchymal signal intensity and edematous signal volume was found only up to 24 hr post challenge. When data corresponding to time points later than 24 hr were included in the analysis, no significant correlation between these parameters was found. The pO2 in the blood assessed before and at several time points after OVA challenge remained constant at around 100 mmHg (data not shown).

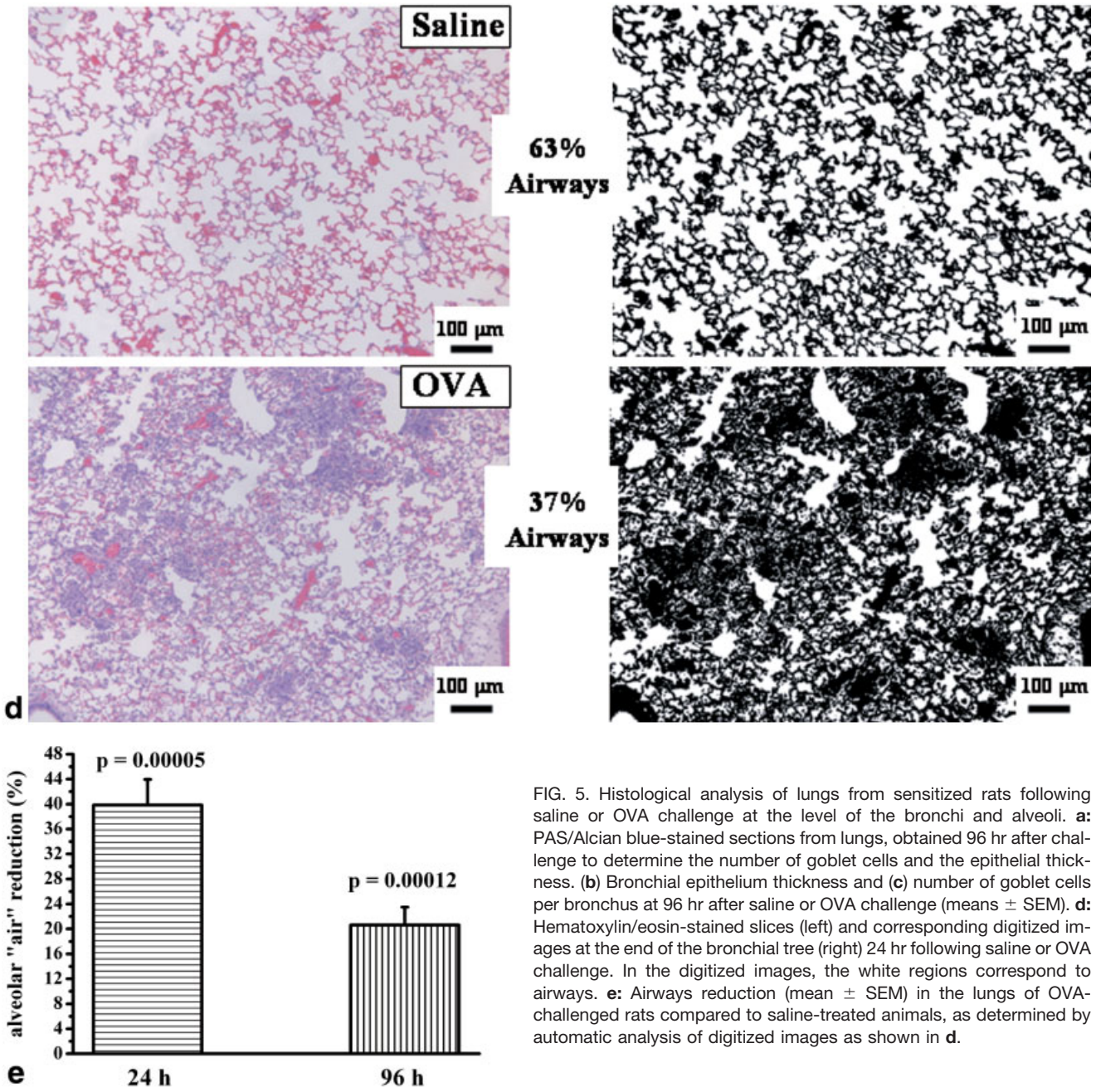


FIG. 5. Histological analysis of lungs from sensitized rats following saline or OVA challenge at the level of the bronchi and alveoli. **a:** PAS/Alcian blue-stained sections from lungs, obtained 96 hr after challenge to determine the number of goblet cells and the epithelial thickness. (**b**) Bronchial epithelium thickness and (**c**) number of goblet cells per bronchus at 96 hr after saline or OVA challenge (means ± SEM). **d:** Hematoxylin/eosin-stained slices (left) and corresponding digitized images at the end of the bronchial tree (right) 24 hr following saline or OVA challenge. In the digitized images, the white regions correspond to airways. **e:** Airways reduction (mean ± SEM) in the lungs of OVA-challenged rats compared to saline-treated animals, as determined by automatic analysis of digitized images as shown in **d**.

Histological analysis of the lungs carried out 96 hr after challenge revealed that the bronchial epithelium thickness in OVA-treated rats was significantly increased by approximately 80% compared to that in animals receiving saline, and the mean number of goblet cells per bronchus was increased by a factor of nearly 12 (Fig. 5a–c). The remodeling caused by OVA instillation resulted in a significant reduction of alveolar airways by 40% and 20% at 24 hr and 96 hr, respectively, after challenge (Fig. 5d and e).

LPS Challenge

Figure 6a displays axial sections through the chest of a rat at different time points relative to i.t. administration of LPS. The course of the lung parenchymal signal following treatment with endotoxin revealed a significant signal decrease 24 hr after the challenge (Fig. 6b). No signal decrease was observed at the same time point when the nitric oxide synthase (NOS) inhibitor, L-NAME (10 mg/kg i.v.), was given 10 min before the challenge. Measurements carried out on control animals (saline-challenged rats, $N = 6$) at the same time points as those represented in Fig. 6b revealed average parenchymal signal intensities ranging between 0.34 and 0.37, with variances of 0.0007–0.005. In accordance with previously published data (8), the volume of edematous signals elicited by LPS was maximum at 48 hr after endotoxin administration (Fig. 6c), and the response was smaller than that

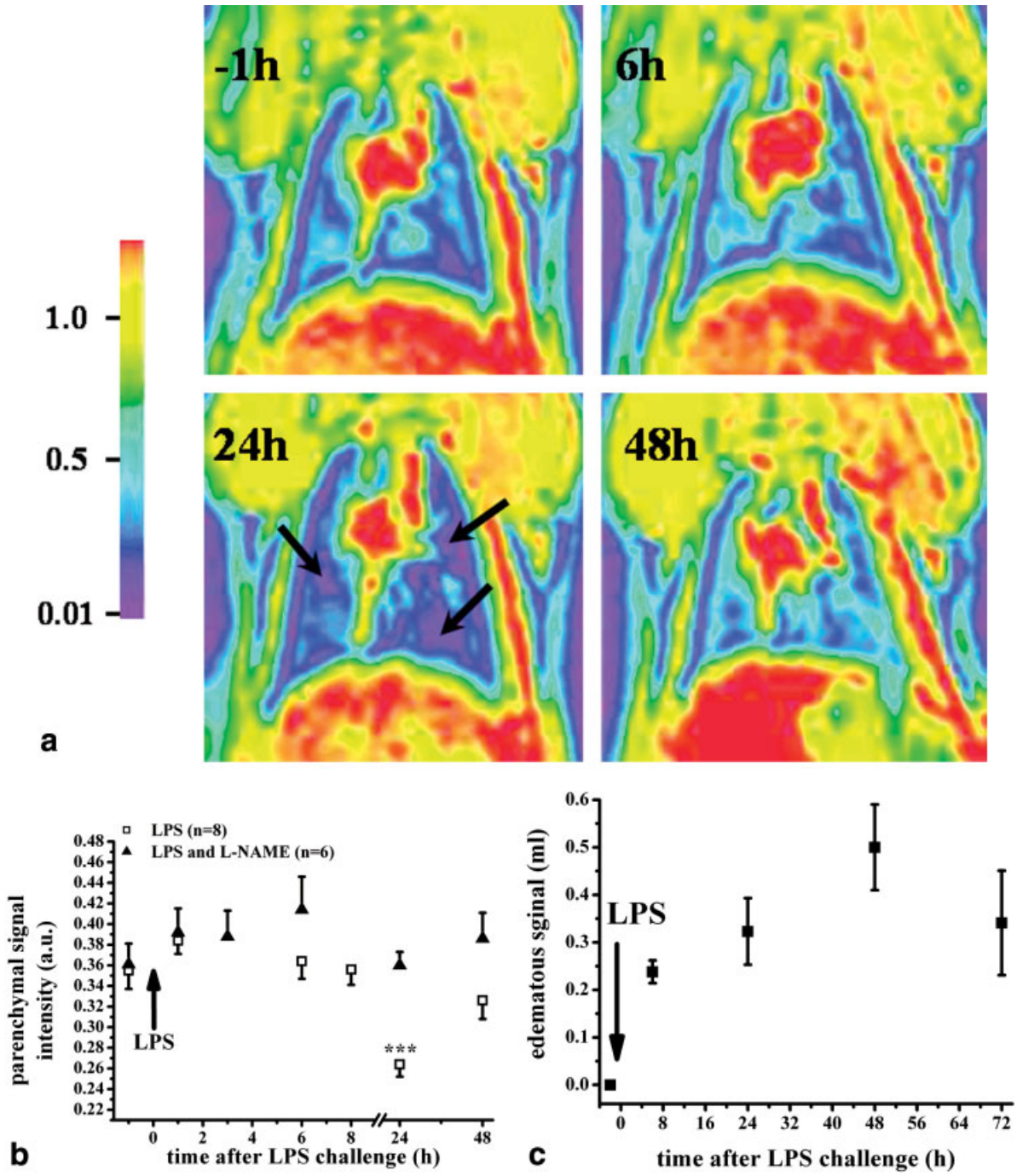


FIG. 6. **a:** Coronal sections acquired through the chest of a rat, before and at several time points after LPS (1.0 mg/kg i.t.) challenge. The position of the slices was chosen to avoid as much as possible regions containing edematous signals. Images are displayed in false color to highlight the drop in parenchymal signal at 24 hr (arrows). The scale on the left side indicates signal intensity in arbitrary units. **b:** Course of the lung parenchymal signal (mean ± SEM) following a challenge with LPS (1 mg/kg i.t.). Some of the animals were pretreated with L-NAME (10 mg/kg i.v.) 10 min before the challenge. The significance level corresponds to comparisons with baseline (BL) signal intensities, before the challenge (***$P < 0.001$). **c:** Time course of the volume of edematous signals (mean ± SEM, $N = 8$) in the lungs of LPS-challenged animals.

following OVA instillation in actively sensitized rats (Fig. 4c). No correlation was detected between the parenchymal signal intensity and the edematous signal volume. Treatment with L-NAME did not result in a decrease of edematous signals detected by MRI.

DISCUSSION

Gas exchange is the major function of the lungs. In order for this process to occur efficiently, the regional pulmonary blood flow (perfusion) and the ventilation in the

lungs must be matched. In diseases of the airways (e.g., asthma and COPD), as well as in the corresponding animal models, lung ventilation can be compromised.

In the past few years, elegant MRI techniques based on the use of hyperpolarized gases have been developed to obtain information on lung ventilation at high spatial resolution in humans and animals (for a recent review, see Ref. 19). Although images of excellent quality are generated, this approach suffers from some drawbacks that could hamper its routine application to pharmacological research involving models of airway disease in small rodents. This disadvantages include the following: 1) gas generation is time-consuming, and thus the total amount of gas available considerably limits the number of animals that can be examined per day; 2) artificial ventilation and often tracheotomy are employed, which restricts the number of times an examination can be repeated on the same animal; 3) invasive manipulations can interfere with the pathophysiology of the disease model; and 4) the technique is expensive.

In our search for a noninvasive and less costly alternative for obtaining information regarding pulmonary function in models of airway disease in small rodents, we investigated the effects of allergen or endotoxin challenge on the behavior of the proton signal from lung parenchyma, as detected with the use of a gradient-echo sequence. Obviously, in regions where edematous signals were present, local ventilation was impaired. Since our aim was to probe the ventilation status of regions deprived of edematous signals, it was this criterion that determined the choice of the slice position. Modulations of the parenchymal signal were expected to be related to airway remodeling or hyporesponsiveness leading to changes in oxygenation levels. Molecular oxygen has a triplet ground state (i.e., two unpaired electrons) and is weakly paramagnetic; thus, it constitutes a source of contrast in MRI. This property has been successfully explored to derive regional ventilation-related information from the human lung (14–18). The main challenge faced by oxygen-enhanced MRI is sensitivity, which is significantly lower than that of ventilation imaging with hyperpolarized gases.

In order to interfere as little as possible with the pathophysiology of the induced inflammation, we performed repeated measurements on spontaneously breathing animals. However, since the sensitivity issue is particularly challenging in small rodents, we carried out the initial studies on artificially ventilated normal rats to probe the ability of the technique to detect the effects of differences in the oxygen content of the administered gas on the parenchymal signal. The difference in partial pressures between the low- and high-oxygen-content gas mixtures led to measurable changes in T_2^*, which were translated into significant changes in parenchymal signal intensity (Figs. 1 and 2). Since the relaxation time T_2^* reflects morphometric features of the microarchitecture of the lung at the alveolar level (20), differences in morphology (e.g., a more prominent bronchial tree on the left lung, or a reduced capability of alveolar expansion resulting from the more prominent presence of the heart on the left semi-thorax (21,22)) could have been responsible for the asymmetry observed in the relaxation times determined in the left and right lungs. On the other hand, this asymmetry might have been accentuated by the direct application of gas into the trachea. Interestingly, when the animals were ventilated and administered a low content of oxygen (21%), the parenchymal signal intensity was significantly lower than that of normal rats (without challenge) breathing freely. This suggests that the ventilation procedure induced a larger lung inflation than that attained by spontaneous respiration (compare Figs. 3, 4b, and 6b). This may also explain the tendentially lower T_2^* values assessed in lungs of artificially ventilated rats compared to those previously reported for spontaneously breathing animals (13). More carefully designed experiments must be carried before we can understand the influence of artificial ventilation on the parenchymal signal.

Presumably, the magnitude of the signal changes observed when the oxygen content of the administered gas was altered in artificially ventilated rats cannot be explained by the paramagnetic effects of molecular oxygen only. Diamagnetic effects in the foam-like structure of the inflated lung cause inhomogeneous line-broadening (equivalent to a shortened free-induction decay (FID)) that is not found in totally collapsed lung or other tissues (23,24). The anomalously short FID is caused by local perturbations in the magnetic field near air–tissue interfaces (24), which are produced by the differences in magnetic susceptibility of tissue and air. Since lung inflation and oxygenation are intrinsically correlated, it is conceivable that the paramagnetic effects of molecular oxygen and the line-broadening caused by an inflated lung add up. Thus, the effects of changes of the oxygen content in tissue upon image contrast are more evident in the lung than in other tissues. Consequently, in our application the outcome effects upon the $1/T_2^*$ relaxation rates may have been amplified, resulting in larger contrast changes in the gradient-echo images than would be expected to be caused solely by the paramagnetic properties of oxygen. Of note, the large signal intensity differences (up to a factor of 2) that arose when the oxygen flow rates were changed have also been observed in T_1-enhanced lung images of humans (25).

Although we did not assess pO_2 directly in the lung, it is reasonable to assume that pO_2 in blood reflects pulmonary oxygenation in normal animals, since for gas exchange to occur efficiently the large amount of ventilation in the lungs must be matched by a correspondingly high perfusion. Thus, the significant inverse correlation between parenchymal signal intensity and pO_2 in blood (Fig. 3) for different oxygen concentrations of the administered gas suggests that the contrast in gradient-echo images of parenchyma is influenced by the oxygenation status of the lungs. This provides a basis for deriving information on ventilation in models of airway diseases. The direct measurement of pO_2 in the lung (e.g., on the basis of the paramagnetic effect of dissolved molecular oxygen, which reduces the ^{19}F T_1 relaxation time of perfluorocarbons administered as aerosols (26)) was beyond the scope of the present work.

Following OVA administration, increased parenchymal signal intensity (in areas devoid of edematous signals) was detected at 6 hr and up to 180 hr after challenge, when edematous signals reflecting inflammation (27) had completely resolved. Histological analysis revealed airway re-

modeling in the lungs of OVA-challenged rats that was characterized as increased bronchial epithelium thickness and smooth muscle area, as well as bronchial goblet-cell hyperplasia. Thus, the increased parenchymal signal in lung images of rats treated with allergen was consistent with a significant reduction of air space as determined histologically, showing an impaired lung ventilation in these animals. Our data further indicate that a ventilation defect remained even after the edematous signals detected by MRI were completely resolved. Although we cannot exclude the possibility that early after challenge, signals reflecting inflammation influenced the observed contrast alteration (despite the careful positioning of the slices and the ROIs to avoid interferences of areas containing edematous signals), airway remodeling was the main reason for the increased parenchymal signal detected at later time points. Taken together, these facts indicate that MRI of the lung parenchyma is sensitive for detecting both early and delayed pathophysiologic structural changes in lung tissue in the allergen model in rats.

The current results are in agreement with previous findings regarding late airway constriction in sensitized BN rats following antigen challenge (28). They also agree with the fact that inflammation in airways leads to pathophysiologic changes in the structure of the tissues, including thickening of the smooth muscle in the airway wall (10), which may influence airway responsiveness (11,12) as well as ventilation, subepithelial fibrosis (29), and goblet cell hyperplasia together with increased mucus accumulation in the airways (30). Detailed studies of remodeling events resulting from allergen exposure carried out in sensitized rats have revealed that epithelial and subepithelial (i.e., fibroblasts and smooth muscle cells) proliferation is increased between 5 and 24 hr after challenge (31,32).

In the second model studied, a significantly decreased parenchymal signal intensity was detected 24 hr after i.t. instillation of LPS (Fig. 5). The effect was abolished by pretreatment with L-NAME, an inhibitor of NOS. Pauwels et al. (33) recently demonstrated that NO may play a role in the inflammatory response elicited by endotoxin. In their study, a period of significant hyporesponsiveness, characterized by reduced pulmonary resistance due to increased airway caliber, followed 9–12 hr after rats were exposed to aerosolized LPS. In the same model, LPS-induced airway hyporesponsiveness was eliminated by L-NAME (34). Moreover, marked expression of inducible NOS in rat macrophages recovered from the airways has been demonstrated 16 hr after local LPS instillation (35). Therefore, the endogenous synthesis of NO (also a potent bronchorelaxant in rats (36)) induced by the endotoxin may have been responsible for an increased oxygenation of the lung tissue, and thus may have contributed to a reduction of the parenchymal signal in the gradient-echo images 24 hr following LPS administration (Fig. 5).

Aside from tissue oxygenation, other factors could have influenced the parenchymal signal intensity in the MR images. For example, the dissolution of oxygen in blood suggests that oxygen-enhanced images may also be dependent on perfusion or blood volume (37). In our approach, average images are acquired over many respiratory cycles to suppress movement artifacts. Although allergen or endotoxin administration can potentially cause inequalities between perfusion and ventilation (38), these mismatches should not have influenced our results, since the acquisition time for an image was very long compared to the cardiac and respiratory cycles. Furthermore, oxygen-content-related T_1 changes (18,25) could not modulate the parenchymal signal because of the short repetition time employed here in the gradient-echo square. Finally, interferences due to repeated anesthesia were ruled out by the observation of a stable parenchymal signal intensity in control rats that were measured at the same time points as allergen- and endotoxin-challenged animals.

In summary, the results presented here imply that proton MRI of the lung parenchyma is a sensitive tool for probing the functional status of the lung following inflammatory stimuli in spontaneously breathing rats. It is essential to carry out such experiments in spontaneously respiring animals to minimize interference with the pathophysiology of the condition. Of special interest is the potential of the technique for assessing the late effects of stimuli related to airway remodeling, when acute inflammation has resolved. The method is thus complementary to recently described MRI approaches that enable the formation of edematous signals after allergen challenge (7,27), or the mucus hypersecretion induced by LPS administration (8), to be followed noninvasively. MRI of lung parenchyma could prove invaluable for providing functional information in studies profiling anti-inflammatory drugs in models of airway diseases (9,39,40).

ACKNOWLEDGMENTS

We thank Dr. John Fozard and Dr. Alexander Trifilieff from the Novartis Institutes for BioMedical Research for their critical reading of the manuscript.

REFERENCES

1. Drazen JM, Takebayashi T, Long NC, De Sanctis GT, Shore SA. Animal models of asthma and chronic bronchitis. Clin Exp Allergy 1999; 29(Suppl 2):37–47.
2. Shapiro SD. Animal models for COPD. Chest 2000;117(5 Suppl 1): 223S–227S.
3. Elwood W, Lotvall JO, Barnes PJ, Chung KF. Characterization of allergen-induced bronchial hyperresponsiveness and airway inflammation in actively sensitized brown-Norway rats. J Allergy Clin Immunol 1991; 88:951–960.
4. Renzi PM, Olivenstein R, Martin JG. Inflammatory cell populations in the airways and parenchyma after antigen challenge in the rat. Am Rev Resp Dis 1993;147:967–974.
5. Watson RW, Redmond HP, Bouchier-Hayes D. Role of endotoxin in mononuclear phagocyte-mediated inflammatory responses. J Leukoc Biol 1994;56:95–103.
6. Yang RB, Mark MR, Gray A, Huang H, Xie MH, Zhang M, Goddard A, Wood WI, Gurney AL, Godowski PJ. Toll-like receptor-2 mediates lipopolysaccharide-induced cellular signalling. Nature 1998;395:284–288.
7. Beckmann N, Tigani B, Ekatodramis D, Borer R, Mazzoni L, Fozard JR. Pulmonary edema induced by allergen challenge in the rat: noninvasive assessment by magnetic resonance imaging. Magn Reson Med 2001;45:88–95.
8. Beckmann N, Tigani B, Sugar R, Jackson AD, Jones G, Mazzoni L, Fozard JR. Non-invasive detection of endotoxin induced mucus hypersecretion in rat lung by magnetic resonance imaging. Am J Physiol Lung Cell Mol Physiol 2002;283:L22–L30.
9. Tigani B, Cannet C, Zurbrügg S, Schaeublin E, Mazzoni L, Fozard JR, Beckmann N. Resolution of the oedema associated with allergic pulmonary inflammation in rats assessed non-invasively by magnetic resonance imaging. Br J Pharmacol 2003;140:239–246.

10. Ebina M, Takahashi T, Chiba T, Motomiya M. Cellular hypertrophy and hyperplasia of airway smooth muscles underlying bronchial asthma: a 3-D morphometric study. Am Rev Respir Dis 1993;148:720–726.
11. Martin JG, Duguet A, Eidelman DH. The contribution of airway smooth muscle to airway narrowing and airway hyperresponsiveness in disease. Eur Respir J 2000;16:349–354.
12. Halayko AJ, Amrani Y. Mechanisms of inflammation-mediated airway smooth muscle plasticity and airways remodeling in asthma. Respir Physiol Neurobiol 2003;137:209–222.
13. Beckmann N, Tigani B, Mazzoni L, Fozard JR. MRI of lung parenchyma in rats and mice using a gradient-echo sequence. NMR Biomed 2001; 14:297–306.
14. Edelman RR, Hatabu H, Tadamura E, Li W, Prasad PV. Noninvasive assessment of regional ventilation in the human lung using oxygen-enhanced magnetic resonance imaging. Nat Med 1996;2:1236–1239.
15. Stock KW, Chen Q, Morrin M, Hatabu H, Edelman RR. Oxygen-enhanced magnetic resonance ventilation imaging of the human lung at 0.2 T and 1.5 T. J Magn Reson Imaging 1999;9:838–841.
16. Hatabu H, Tadamura E, Chen Q, Stock KW, Li W, Prasad PV, Edelman RR. Pulmonary ventilation: dynamic MRI with inhalation of molecular oxygen. Eur J Radiol 2001;37:172–178.
17. Nakagawa T, Sakuma H, Murashima S, Ishida N, Matsumura K, Takeda K. Pulmonary ventilation-perfusion MR imaging in clinical patients. J Magn Reson Imaging 2001;14:419–424.
18. Jakob PM, Hillenbrand CM, Wang T, Schultz G, Hahn D, Haase A. Rapid quantitative lung ^{1}H T_1 mapping. J Magn Reson Imaging 2001; 14:795–799.
19. Möller HE, Chen XJ, Saam B, Hagspiel KD, Johnson GA, Altes TA, de Lange EE, Kauczor H-U. MRI of the lungs using hyperpolarized noble gases. Magn Reson Med 2002;47:1029–1051.
20. Case TA, Durney CH, Ailion DC, Cutillo AG, Morris AH. A mathematical model of diamagnetic line broadening in lung tissue and similar heterogeneous systems: calculations and measurements. J Magn Reson 1987;73:304–314.
21. Burri PA, Dhaly J, Weibel ER. The post-natal growth of the rat lung: I morphometry. Anat Rec 1973;178:711–730.
22. Nardell EA, Brody JS. Determinants of mechanical properties of rat lung during postnatal development. J Appl Physiol 1982;53:140–148.
23. Blatter DD, Morris AH, Ailion DC, Cutillo AG, Case TA. Asymmetric spin echo sequences. A simple new method for obtaining NMR 1H spectral images. Invest Radiol 1985;20:845–853.
24. Morris AH, Blatter DD, Case TA, Cutillo AG, Ailion DC, Durney CH, Johnson SA. A new nuclear magnetic resonance property of lung. J Appl Physiol 1985;58:759–762.
25. Mai VM, Liu B, Li W, Polzin J, Kurucay S, Chen Q, Edelman RR. Influence of oxygen flow rate on signal and T_1 changes in oxygen-enhanced ventilation imaging. J Magn Reson Imaging 2002;16:37–41.
26. Thomas SR, Gradon L, Pratsinis SE, Pratt RG, Fotou GP, McGoron AJ, Podgorski AL, Millard RW. Perfluorocarbon compound aerosols for delivery to the lung as potential 19F magnetic resonance reporters of regional pulmonary pO2. Invest Radiol 1997;32:29–38.
27. Tigani B, Schaeublin E, Sugar R, Jackson AD, Fozard JR, Beckmann N. Pulmonary inflammation monitored non-invasively by MRI in freely breathing rats. Biochem Biophys Res Commun 2002;292:216–221.
28. Nagase T, Moretto A, Dallaire MJ, Eidelman DH, Martin JG, Ludwig MS. Airway and tissue responses to antigen challenge in sensitized brown Norway rats. Am J Respir Crit Care Med 1994;150:218–226.
29. Roche WR, Beasley R, Williams JH, Holgate ST. Subepithelial fibrosis in the bronchi of asthmatics. Lancet 1989;1:520–524.
30. Aikawa T, Shimura S, Sasaki H, Ebina M, Takishima T. Marked goblet cell hyperplasia with mucus accumulation in the airways of patients who died of severe asthma attack. Chest 1992;101:916–921.
31. Cui ZH, Skoogh BE, Pullerits T, Lotvall J. Bronchial hyperresponsiveness and airway wall remodeling induced by exposure to allergen for 9 weeks. Allergy 1999;54:1074–1082.
32. Palmans E, Kips JC, Pauwels RA. Prolonged allergen exposure induces structural airway changes in sensitized rats. Am J Respir Crit Care Med 2000;161:627–635.
33. Pauwels RA, Kips JC, Peleman RA, van der Straeten ME. The effect of endotoxin inhalation on airway responsiveness and cellular influx in rats. Am Rev Respir Dis 1990;141:540–545.
34. Kips JC, Lefebvre RA, Peleman RA, Joos GF, Pauwels RA. The effect of a nitric oxide synthase inhibitor on the modulation of airway responsiveness in rats. Am J Respir Crit Care Med 1995;151:1165–1169.
35. Kobzik L, Bredt DS, Lowenstein CJ, Drazen J, Gaston B, Sugarbaker D, Stamler JS. Nitric oxide synthase in human and rat lung: immunocytochemical and histochemical localization. Am J Respir Cell Mol Biol 1993;9:371–377.
36. Abderrahmane A, Salvail D, Dumoulin M, Garon J, Cadieux A, Rousseau E. Direct activation of K_{Ca} channel in airway smooth muscle by nitric oxide: involvement of a nitrothiosylation mechanism? Am J Respir Cell Mol Biol 1998;19:485–497.
37. Mai VM, Liu B, Polzin JA, Li W, Kurucay S, Bankier AA, Knight-Scott J, Madhav P, Edelman RR, Chen Q. Ventilation-perfusion ratio of signal intensity in human lung using oxygen-enhanced and arterial spin labeling techniques. Magn Reson Med 2002;48:341–350.
38. Lagerstrand L, Larsson K, Ihre E, Zetterstrom O, Hedenstierna G. Pulmonary gas exchange response following allergen challenge in patients with allergic asthma. Eur Respir J 1992;5:1176–1183.
39. Tigani B, di Padova F, Zurbrügg S, Revesz L, Fozard JR, Beckmann N. Effects of a mitogen-activated protein kinase inhibitor on allergic airways inflammation in the rat studied by magnetic resonance imaging. Eur J Pharmacol 2003;482:319–324.
40. Beckmann N, Tigani B, Mazzoni L, Fozard JR. Magnetic resonance imaging of the lung provides potential for preclinical evaluation of drugs. Trends Pharmacol Sci 2003;24:550–554.